WORLD CONFERENCE ON TIMBER ENGINEERING 2025
BRISBANE, AUSTRALIA
Advancing Timber for the Future Built Environment

NUMERICAL SIMULATION OF WOODEN DOWELS UNDER COMPRESSION

Inayat Ullah Khan [1], Mahbube Subhani [2], Kazem Ghabraie [3], Mahmud Ashraf [4]

ABSTRACT: The compression behavior of wooden dowels plays a critical role in timber structures, particularly in dowel-laminated timber (DLT), as it influences load transfer efficiency, joint stiffness, material compatibility, and structural durability while enabling sustainable, adhesive-free designs. The performance of dowels under compression perpendicular to the grain is particularly significant due to its impact on joint embedment behavior. Bearing strength is a key parameter in timber connection design and is used as an input for single and double shear connection analyses in Eurocode 5 and the National Design Specification (NDS) yield limit equations. However, due to their round cross-section and small transverse dimensions, existing design codes do not provide specific recommendations for compression testing of dowels. Additionally, the high variability in timber properties makes numerical modeling of post-peak behavior challenging, particularly in compression. Unlike shear and tension, which exhibit brittle post-peak softening that can be captured numerically, compression perpendicular to the grain results in a stress-strain response characterised by densification without a distinct drop. To date, no study has successfully modeled post-peak hardening behavior in compression perpendicular to the grain. Therefore, this research investigates the applicability of the continuum damage mechanics-based constitutive model, MAT-143 in LS-DYNA, for capturing post-peak hardening in compression perpendicular to the grain. Furthermore, MAT-143 is also employed to model pre-peak nonlinear hardening behavior in compression parallel to the grain. To address this gap, Tasmanian Oak dowels were experimentally tested and subsequently numerically modeled using MAT-143 for both parallel and perpendicular compression.

KEYWORDS: LS-DYNA, wooden dowels, Tasmanian Oak, compression, MAT-143

1 – INTRODUCTION

A timber-timber connection is constructed using either mechanical fasteners or adhesives. The durability concerns associated with metal fasteners, the emission of toxic gases from adhesives—particularly formaldehyde—and the complex application procedures of adhesives, along with their limitations in automated wood processing, have directed research interest toward wooden dowels [1]. With the compatibility of Computer Numerical Control (CNC) technology with dowel-laminated timber (DLT), StructureCraft, a leading DLT manufacturer in North America, has established the world's largest automated DLT production line.

Dowel-laminated timber (DLT) is rapidly gaining popularity, with its application observed in various projects across North America and Europe. In recent years, DLT has been extensively studied, as evidenced by several research investigations [1], [2], [3], [4]. Wooden dowels provide a more sustainable alternative to adhesives and eliminate the need for surface preparation required in adhesive bonding. Additionally, they help mitigate delamination issues caused by weak bonding in dense wood, making them a subject of increasing research interest [5]. The design of timber-timber connections requires bending strength and embedment strength as key input parameters. Literature suggests that, unlike metal fasteners—where embedment occurs solely in the timber—embedment failure in wooden dowel connections occurs in both the dowel and timber layers [6]. Since embedment behaviour is directly linked to the compression response of wood, understanding the compression behaviour of wooden dowels is essential.

Australia's forest cover spans approximately 134 million hectares, categorised into native forests, commercial plantations, and other forest types. Native forests account for nearly 132 million hectares, with approximately 77% consisting of hardwood species [7]. Given this vast forest resource, its potential for various applications cannot be overlooked. Hardwood, with its superior mechanical properties, presents a viable option for use as dowels in timber connections.

In this study, Australian hardwood dowels, specifically Tasmanian Oak (TO), were experimentally tested under compression both parallel and perpendicular to the grain. The test setup was developed based on initial experimental trials and numerical simulations using LS-DYNA. Experimental data were validated against numerical

[1] Inayat Ullah Khan, School of Engineering, Deakin University, Waurn Ponds, VIC, Australia, inayat.khan@deakin.edu.au

[2] Mahbube Subhani, School of Engineering,Deakin University,Waurn Ponds, VIC, Australia, mahbube.subhani@deakin.edu.au

[3] Kazem Ghabraie, School of Engineering, Deakin University, Waurn Ponds, VIC, Australia, k.ghabraie@deakin.edu.au

[4] Mahmud Ashraf, School of Engineering, Deakin University, Waurn Ponds, VIC, Australia, mahmud.ashraf@deakin.edu.au

https://doi.org/10.52202/080513-0350

modelling employing the MAT-143 material model. Conventional timber design relies on elastic modulus and strength parameters, which may not be suitable for applications—particularly in connections—where post-peak response is critical. To fully utilize the load-carrying capacity of timber, a fracture-based approach is necessary, accounting for post-elastic behaviour. To capture this response, MAT-143 in LS-DYNA was used to validate the experimental results. A mesh sensitivity analysis was performed to ensure a stable response and determine the optimal mesh size. Limited studies exist on the mechanical behaviour of wooden dowels, and research on TO dowels is particularly scarce. Moreover, no studies have explored the numerical modelling of their post-elastic behaviour in compression perpendicular to the grain, highlighting a significant research gap that requires investigation.

2 – BACKGROUND

This study consists of two parts. First, Australian hardwood dowels, specifically TO with a diameter of 19 mm, were experimentally tested under compression both parallel and perpendicular to the grain. Since no standardized compression testing protocol exists for wooden dowels, test specimens were prepared based on relevant literature, and standards and tested under a displacement-controlled environment. The second part involves the application and evaluation of the continuum damage mechanics-based constitutive material model, MAT-143 in LS-DYNA, for simulating the post-elastic behaviour of dowels. The results from experimental testing and numerical modelling are compared and discussed in the following sections.

3 – EXPERIMENTAL SETUP

The dowels, initially 2 meters in length, were cut to the required sizes. Moisture content (MC) was first measured using a protimeter and then adjusted by conditioning the dowels in a controlled chamber under standard conditions to achieve an MC of approximately 12%. All dowels were tested with an MC in the range of 12 ± 0.65%. The density of the dowels was determined to be 650 kg/m³, while the oven-dry specific gravity of TO was found to be 0.631, which falls within the range recommended by ASTM D8023-23 [8] for wooden dowels.

Prior to testing, the top and bottom surfaces were cleaned and machined to be parallel to minimize loading eccentricity. ASTM D8023-23 specifies that the slope of the grain should not deviate by more than 1 in 20 and that dowels should be free from knots, shakes, and splits. All specimens were inspected and confirmed to meet these requirements [8]. A TO dowel specimen is shown in Figure 1.

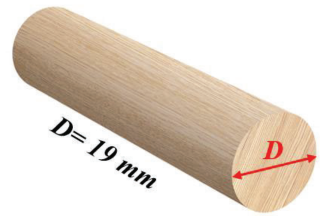

Figure 1 Tasmanian Oak dowel

Tasmanian Oak dowels with a diameter of 19 mm were tested under compression parallel to the grain. Due to the limited transverse dimensions of the dowels, the specimen sizes recommended by ASTM D143 and EN 408 were not applicable. Instead, various dowel lengths were numerically modelled to determine a suitable length that would mitigate buckling issues. The final length was selected based on a rational reduction of dimensions as recommended by ASTM D143 and verified using Euler's buckling formulation. A dowel length of 35 mm was identified as the most suitable, as it did not exhibit any signs of buckling. The central 30 mm region was designated for strain measurement, with 2.5 mm left at both ends to account for potential damage zones, which could influence strain measurements, as suggested by previous research [9]. The elastic modulus in compression parallel to the grain was determined within the elastic range. Testing was conducted in a displacement-controlled environment, with the crosshead moving at a speed of 0.20 mm/min, following ASTM D143. Strain measurements were obtained using a non-contact video extensometer (NVE). Due to variations in laboratory lighting conditions, the NVE employs a patented cross-polarized lighting system, ensuring consistent performance independent of ambient lighting. To facilitate strain tracking, two reference dots were marked on the dowel using white paint. During testing, the NVE tracked these dots and used their displacement to compute strain. The NVE setup is shown in Figure 2.

In compression perpendicular to the grain, the specimen sizes recommended by EN 408 and ASTM D143 could not be applied due to the limited transverse dimensions of the dowels. Furthermore, the rounded shape of the dowels makes testing in pure compression perpendicular to the grain challenging. During compression, the dowel experiences tensile stresses in other axes due to biaxial stress, which affects the overall stress distribution. To address this issue, the top surface of the dowels was removed to create a flat loading surface. The thickness of the flat surface was 10 mm, the dowel length was 50 mm, and the strain was measured between the top and bottom surfaces over a length of 16 mm. In case of compression perpendicular to grain, the graph has an increasing slope, and it becomes difficult to determine the peak load.

https://doi.org/10.52202/080513-0350

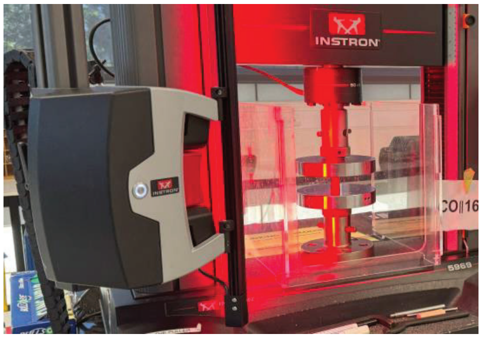

Figure 2. Test setup including specimen and NVE

Standards provided various recommendations to estimate $F_{c\text{-}90\text{-}max}$ such as EN 408 and EN 1995-1-1 take it at 0.01h, ASTM D143-14 at 1 mm, AS/NZ at 2 mm and ISO 13910 at 2 mm. EN 408 was used, where a line was drawn parallel to the elastic portion of the force-deformation curve at a deformation of 0.01h. A compression load was applied at a rate of 1 mm/min in case of compression perpendicular the grain. The modulus of elasticity perpendicular to grain ($E_{90\text{-}com}$) was determined using EN 408 using Equation (1). The terms are defined in Figure 3, and the test setup for compression perpendicular to the grain is shown in Figure 4.

$$E_{com-90} = \frac{(F_{40} - F_{10})h}{(\Delta_{40} - \Delta_{10})A} \tag{1}$$

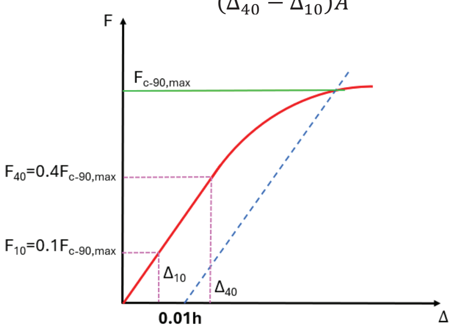

Figure 3 Force-deformation curve

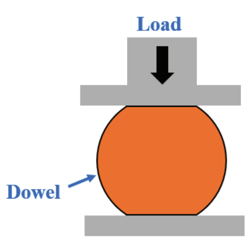

Figure 4 Compression perpendicular to grain

4 –MODELING PROTOCOL

To numerically model wooden dowels, the finite element analysis software LS-DYNA was used. LS-DYNA was chosen because it includes built-in material models specifically designed for wood, whereas ABAQUS and ANSYS do not have dedicated timber models. In ABAQUS and ANSYS, researchers must develop user-defined subroutines or custom codes, which is complex and requires specialized programming knowledge.

LS-DYNA offers over 250 material models, among which MAT-143 was selected for this study. MAT-143 is specifically developed for timber, unlike other models in LS-DYNA that are primarily designed for fiber-reinforced composites. While alternative models can be applied to timber, they require numerous input parameters that are often difficult to obtain for wood materials.

Material model MAT-143 in LS-DYNA was used to model TO dowels under compression both parallel and perpendicular to the grain. This is a transversely isotropic model, in which the tangential and radial properties are assumed to be the same. This assumption is reasonable for timber, as the differences between radial and tangential properties are relatively small compared to the longitudinal direction.

Nine elastic constants are required to characterize the elastic stiffness matrix of an orthotropic material: E_{LL}, E_{RR}, E_{TT}, G_{LR}, G_{LT}, G_{RT}, υ_{LR}, υ_{LT} and υ_{RT}. Here, E represents elastic modulus, G is the shear modulus, and υ is the poison ratio. The subscripts L, R, and T refer to the longitudinal, radial, and tangential directions, respectively. The three poison's ratios υ_{RL}, υ_{TL} and υ_{TR} can be obtained from equation (2).

$$\frac{\upsilon_{ij}}{E_i} = \frac{\upsilon_{ji}}{E_j} \quad where\ i, j = 1, 2, 3 \tag{2}$$

Under the transversely isotropic assumption, the number of independent elastic constants is reduced to five: E_{LL}, E_{RR}=E_{TT}, G_{LR}= G_{LT}, G_{RT}, υ_{LR}= υ_{LT}. The sixth constant, υ_{RT}, is determined using the following relationship:

$$\upsilon_{RT} = \frac{E_{TT} - 2G_{RT}}{2G_{RT}} \tag{3}$$

For simplicity, the longitudinal (LL), tangential (TT), and radial (RR) directions are represented by L, T, and R, respectively, in stress presentation. In MAT-143, the perpendicular directions (radial and tangential) are collectively represented by T.

MAT-143 requires various input parameters, including density, strength properties, elastic moduli, softening parameters, hardening parameters, fracture energies, and damage parameters. The elastic moduli define the initial slope of the stress-strain curve.

Non-linearity in compression is captured through hardening parameters, which translates the yield surface until it aligns with the ultimate yield surface. Two hardening parameters, C and N, are defined separately for parallel ($C_{\parallel}$, $N_{\parallel}$) and perpendicular ($C_{\perp}$, $N_{\perp}$) modes. The parameter N controls the point at which the stress-strain or load-deflection curves deviate from linearity.

The parameter C controls the rate of hardening; higher values produce rapid hardening, while lower values result

https://doi.org/10.52202/080513-0350

in gradual hardening. These parameters, represented in LS-DYNA as NPAR, CPAR, NPER, and CPER, are determined from experimental data. For example, if $N_\parallel$=0.4, non-linearity will begin at (1-0.4)=0.6 (i.e., 60%) of the compressive strength value (X_C). Additionally, the GHARD parameter, which governs perfect plasticity override, is fitted to the slope of the stress-strain curve and depends on the post-elastic response. The translation of yield surfaces is illustrated in Figure 5.

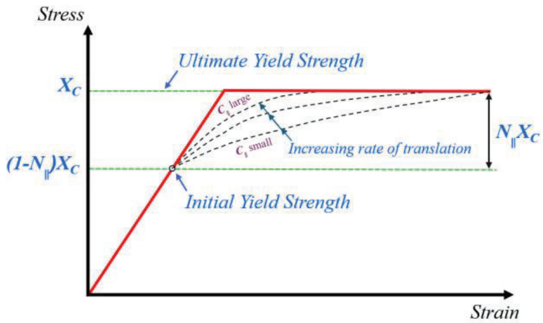

Figure 5 Yield surface translation in compression

The failure surface definition for compression testing incorporates hardening parameters. The yield surfaces for parallel and perpendicular failure modes are expressed as follows:

$$f_\parallel = \frac{\sigma_{11}{}^2}{X_c{}^2(1-N_\parallel)^2} + \frac{(\sigma_{12}{}^2+\sigma_{13}{}^2)}{S_\parallel{}^2} - 1 \quad \sigma_{11} < 0 \qquad (4)$$

$$f_\perp = \frac{(\sigma_{22}+\sigma_{33})^2}{Y_c{}^2(1-N_\perp)^2} + \frac{(\sigma_{23}{}^2-\sigma_{22}\sigma_{33})}{S_\perp{}^2} - 1 \quad \sigma_{22}+\sigma_{33} < 0 \qquad (5)$$

Wood failure in the parallel direction is catastrophic, rendering the material completely unusable. Fiber failure eliminates the wood's ability to carry any load, both in the parallel and perpendicular directions, leading to uniform degradation of all six stress components. In contrast, failure in the perpendicular direction only affects the perpendicular stress components, as the fibres in the parallel direction can still bear loads despite perpendicular failure.

Material model MAT-143 in LS-DYNA requires the damage parameters $d_{max\parallel}$ and $d_{max\perp}$ as input. The default values are $d_{max\parallel} = 0.9999$ and $d_{max\perp} = 0.9900$. These values are set slightly below 1 to prevent computational issues associated with zero stiffness at $d_{max} = 1$. Since element erosion is more severe in the parallel direction under loading along the grain, $d_{max\parallel}$ is set closer to 1 than $d_{max\perp}$. Retaining 1% of the original strength and stiffness helps mitigate numerical instabilities.

The remaining properties of Tasmanian Oak were experimentally determined, and the findings are currently under review for publication. Due to the limited availability of fracture properties for Tasmanian Oak in the literature, these properties were extracted through an inverse approach, combined with studies from [10], [11]. The softening parameters B (BFIT) and D (DFIT) were derived by fitting experimental curves.

4.1 Post-Peak non-linearity

The translation of yield surfaces is shown in Figure 5. Back stress, denoted by α, is a variable that define the translation of yield surfaces. At initial yield strength, the $\alpha = 0$ and at the ultimate yield strength, it is $\alpha = -N_\parallel X_c$. The back stress reached to maximum at ultimate yield strength, presenting the maximum translation of yield surface in free space. The growth of the back stress is governed by a hardening rule based on stress. The incremental back stress is defined as.

$$\Delta\alpha = CG(\sigma - \alpha)\Delta\dot{\varepsilon}\Delta t \qquad (6)$$

The stresses update with hardening until α become maximum and stress reach the ultimate yield strength σ^F.

$$\sigma = \overline{\sigma} + \alpha \qquad (7)$$

$$\sigma^F = \overline{\sigma} + \alpha^{max} \qquad (8)$$

Where
C= Rate of translation
G = limiting function that ensures yield surface does not exceed the ultimate surface
$\sigma - \alpha$ = Reduced stress defining the direction of translation.
$\Delta\dot{\varepsilon}$= Effective strain rate increment
Δt= time step
$\overline{\sigma}$ = Stress at initial yield (no hardening yet)

The above terms are internally calculated by LS-DYNA. The *G* control the motion of the yield surfaces so that it does not go outside the ultimate surface. The value of *G*=1 at initial yield where $\alpha = 0$. *G*= 1 at ultimate yield surface where $\alpha = -N_\parallel \sigma_{11}{}^F$. This means that *G* control the growth of the backstress as ultimate yield surfaces approaches. However, when post-peak hardening is activated, then minimum value is kept at *G*= G_{hard} instead of *G*=0. The ultimate yield surface is defined as

$$\sigma_{11}{}^F = X_c\sqrt{1 - \frac{I_4}{S_\parallel^2}} \qquad (9)$$

In case of compression only, the $\sigma_{11}{}^F = X_c$. The same can be for perpendicular modes.

The MAT-143 data card is presented in table 1. The material properties in LS-DYNA were input using the units GPa, msec, mm, kg/mm³, and kN. This unit system was chosen because using MPa results in significantly larger numerical values, which can increase computational time. For a more detailed understanding of material model MAT-143, readers are encouraged to consult the LS-DYNA manuals [12], [13].

https://doi.org/10.52202/080513-0350

Table 1 Material properties of Tasmanian Oak for MAT-143

Symbols	Mechanical property	Parallel	Perpendicular	Unit
RO	Mass density	650×10-9	650×10-9	kg/mm^3
EL	Parallel normal modulus	4.60298	4.60298	GPa
ET	Perpendicular normal modulus	0.22119	0.22119	GPa
GLT=GLR	Parallel shear modulus	1.6280	1.6280	GPa
GTR	Perpendicular shear modulus	0.410	0.410	GPa
PR	Parallel major Poisson's ratio	0.17600	0.17600	-
XT	Parallel tensile strength	0.14262	0.14262	GPa
XC	Parallel compressive strength	0.06930	0.06930	GPa
YT	Perpendicular tensile strength	0.00433	0.00433	GPa
YC	Perpendicular compressive strength	0.00591	0.00591	GPa
SXY	Parallel shear strength	0.01143	0.01143	GPa
SYZ	Perpendicular shear strength	0.01143	0.01143	GPa
GF1‖	Parallel fracture energy in tension	0.0200	0.0200	GPa.mm
GF2‖	Parallel fracture energy in shear	0.1115	0.1115	GPa.mm
BFIT	Parallel softening parameter.	300	300	-
DMAX‖	Parallel maximum damage.	0.9999	0.9999	-
GF1P	Perpendicular fracture energy in tension	0.00115	0.00115	GPa.mm
GF2P	Perpendicular fracture energy in shear	0.00220	0.00220	GPa.mm
DFIT	Perpendicular softening parameter	300	300	-
DMAXP	Perpendicular maximum damage	0.99	0.99	-
NPAR	Parallel hardening initiation	0.400	0.400	-
CPAR	Parallel hardening rate	250	400	-
NPER	Perpendicular hardening initiation	0.500	0.500	-
CPER	Perpendicular hardening rate	70.0	200	-
GHARD	Perfect plasticity override	0	0.124	-

Continuum Damage Mechanics-based models are highly sensitive to element size and mesh uniformity. Ensuring a uniform mesh is crucial for an even distribution of fracture energy across all elements. Therefore, specimens loaded in both parallel and perpendicular directions were tested with various mesh sizes, as shown in Figure 6. A 0.5 mm mesh provided accurate results but was computationally expensive. A 1 mm mesh was adopted as a balance between accuracy and efficiency for both loading cases. The strength convergence results are presented in Figure 7.

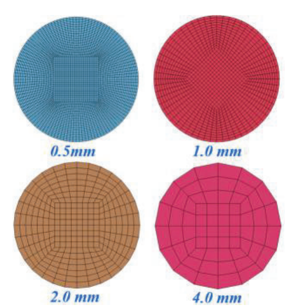

Figure 6 Mesh Sizes

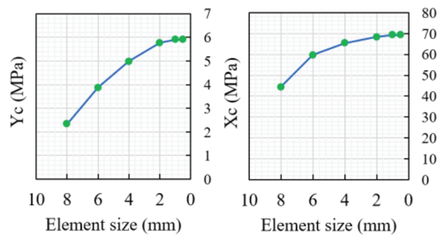

Figure 7 Strength vs element size

5 – RESULTS

The stress-strain curves for all five specimens, obtained from experimental testing and numerical modelling using LS-DYNA with MAT-143, are presented in Figures 8 and 9 for compression parallel and perpendicular to the grain, respectively. The key results extracted from these stress-strain curves, including strength and elastic modulus values, are summarized in table 2 for compression parallel to the grain and table 3 for compression perpendicular to the grain.

The MAT-143 model accurately captured the stress-strain behaviour in the linear, hardening, and peak regions. However, in the case of compression parallel to the grain, some deviation was observed in the post-peak region. This discrepancy arises because MAT-143 requires fracture energy as input for tension and shear but does not account for fracture energy in compression. As a result, the model cannot simulate softening behaviour in compression. Nevertheless, in timber-timber connections with dowels, the dowel does not typically reach its full compression capacity along the grain. Therefore, the response up to peak stress is sufficient for modelling purposes.

For compression perpendicular to the grain, MAT-143 closely matched the experimental results across all regions, including the linear, hardening, peak, and post-peak hardening phases. The post-peak hardening behaviour in compression perpendicular to the grain can be attributed to the densification of the dowel as strain increases, a phenomenon that MAT-143 successfully captures. This capability represents a significant contribution, as modelling compression perpendicular to the grain is rarely addressed in the literature. The compressive strength of Tasmanian Oak was found to be 69.30 MPa along the grain and 5.91 MPa perpendicular to the grain.

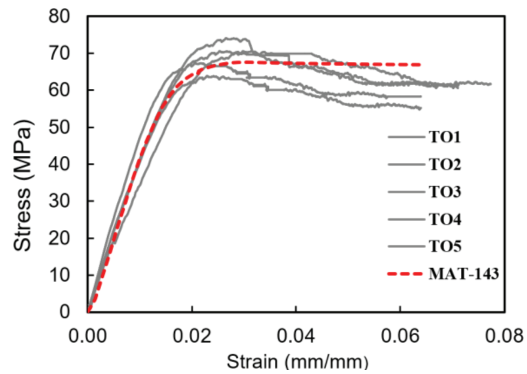

Figure 8 Stress-strain curve for compression along grain

Table 2 Results from compression along grain

ID	XC (MPa)	$Ec_{\parallel}$ (MPa)
TO1	67.40	5415.05
TO2	63.87	4535.76
TO3	70.58	4542.14
TO4	70.58	3767.48
TO5	74.08	4754.49
Average	**69.30**	**4602.98**
COV %	**5.55**	**12.80**
MAT-143	67.57	4199.03
Experimental/Numerical	1.03	1.10

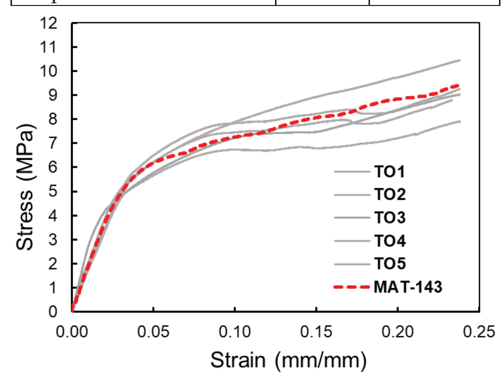

Figure 9 Stress-strain curve for compression perpendicular to grain

Table 3 Results from compression perpendicular to grain

ID	YC (MPa)	$Ec_{\perp}$ (MPa)
TO1	5.39	265.44
TO2	6.50	176.72
TO3	5.44	271.07
TO4	6.08	171.31
TO5	6.12	221.40
Average	**5.91**	**221.19**
COV %	**8.09**	**21.34**
MAT-143	6.07	203.38
Experimental/Numerical	0.97	1.09

https://doi.org/10.52202/080513-0350

The failure modes of the dowels are presented in Figure 10. In compression along the grain, the dowels primarily failed due to shearing and crushing. In contrast, under compression perpendicular to the grain, the dowels exhibited densification with increasing load. Some cracks were observed in the curved portions of the dowels, which may have resulted from tensile stresses induced during perpendicular-to-grain testing. The stress distribution for loading perpendicular to the grain is illustrated in Figure 11.

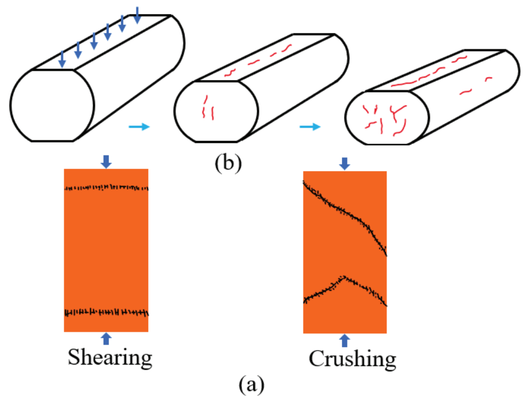

Figure 10 Dowel failure under compression (a) parallel (b) perpendicular to grain

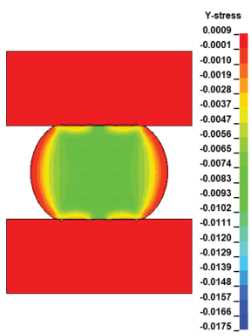

Figure 11 Stress distribution obtained using numerical simulation

6 – CONCLUSION

In this study, Australian hardwood dowels, specifically TO, were experimentally tested under compression and numerically simulated using the CDM-based model MAT-143. The objective was to capture the post-elastic response, which is often overlooked in conventional design. The key conclusions drawn from this study are as follows:

- A circular dowel section with flattened top and bottom surfaces can be used to determine compressive strength in the perpendicular-to-grain direction. The presence of flat surfaces provides a more uniform stress distribution compared to a fully circular section.
- The compressive strength of TO was found to be 69.30 MPa parallel to the grain and 5.91 MPa perpendicular to the grain. The corresponding elastic modulus values were 4602.98 MPa and 221.19 MPa, respectively.
- MAT-143 successfully captured the perfectly plastic override behaviour of dowels under compression perpendicular to the grain, where stress continues to increase with strain. The hardening parameter G_{HARD} in LS-DYNA is a critical input that determines the slope of the stress-strain curve beyond the peak strength.
- While MAT-143 cannot model post-peak softening in compression due to the absence of fracture energy as an input parameter, it can approximate behaviour close to perfectly plastic. However, this limitation is not critical for timber-timber connections, as dowels rarely reach their ultimate compression capacity along the grain in practical applications.

This research provides valuable insights for researchers, manufacturers, and practitioners involved in the design of dowel-based timber connections. The proposed numerical model can be used for finite element modelling of wooden dowels and serves as a useful tool for further studies on their mechanical characterisation. Future research could explore the use of alternative LS-DYNA models, such as MAT-213 and MAT-261, to better capture the post-elastic behaviour of dowels under various loading conditions.

REFERENCES

[1] A. Sotayo *et al.*, "Review of state of the art of dowel laminated timber members and densified wood materials as sustainable engineered wood products for construction and building applications," *Dev. Built Environ.*, vol. 1, p. 100004, Feb. 2020, doi: 10.1016/j.dibe.2019.100004.

[2] G. Bruzzone, D. Godoy, S. Quagliotti, S. Arrejuría, S. Böthig, and L. Moya, "Experimental Investigation on Dowel Laminated Timber Made of Uruguayan Fast-Grown Species," *Forests*, vol. 14, no. 11, Art. no. 11, Nov. 2023, doi: 10.3390/f14112215.

[3] L. Giordano, M. Derikvand, and G. Fink, "Bending Properties and Vibration Characteristics of Dowel-Laminated Timber Panels Made with Short Salvaged Timber Elements," *Buildings*, vol. 13, no. 1, Art. no. 1, Jan. 2023, doi: 10.3390/buildings13010199.

[4] M. Oudjene, V.-D. Tran, and M. Khelifa, "Cyclic and monotonic responses of double shear single dowelled timber connections made of hardwood species: Experimental investigations," *Constr. Build. Mater.*, vol. 132, pp. 188–195, Feb. 2017, doi: 10.1016/j.conbuildmat.2016.11.127.

[5] W. Dong, Z. Wang, J. Zhou, and M. Gong, "Experimental study on bending properties of cross-laminated timber-bamboo composites," *Constr. Build. Mater.*, vol. 300, p. 124313, Sep. 2021, doi: 10.1016/j.conbuildmat.2021.124313.

[6] J. Ou, W. Long, H. Jin, Z. Li, X. Sun, and M. He, "Embedment strength of dowel-type fasteners for the case of cross-laminated timber plane side insertion," *Structures*, vol. 51, pp. 1257–1267, May 2023, doi: 10.1016/j.istruc.2023.03.121.

[7] Department of Agriculture, Fisheries and Forestry, "Australia's forests – overview - DAFF." Accessed: Jun. 25, 2024. [Online]. Available: https://www.agriculture.gov.au/abares/forestsaustralia/australias-forests/profiles/australias-forests-2019

[8] D07 Committee, *ASTM D8023-23 Specification for Round Wood Dowels (Pegs) for Use in Wood Construction*, 100 Barr Harbor Drive, PO Box C700, West Conshohocken, PA, 19428-2959 USA., 2023. doi: 10.1520/D8023-23.

[9] M. Totsuka, R. Jockwer, K. Aoki, and M. Inayama, "Experimental study on partial compression parallel to grain of solid timber," *J. Wood Sci.*, vol. 67, no. 1, p. 39, May 2021, doi: 10.1186/s10086-021-01972-w.

[10] G. B. D. B. Boli, M.-G. Tétreault, M. Oudjene, D. Coutellier, H. Naceur, and M. Fafard, "Numerical modelling of the structural response of a novel hybrid densified wood filled-aluminium tube dowel for structural timber connections," *Compos. Struct.*, vol. 334, p. 117987, Apr. 2024, doi: 10.1016/j.compstruct.2024.117987.

[11] I. El Houjeyri, V. D. Thi, M. Oudjene, L.-M. Ottenhaus, M. Khelifa, and Y. Rogaume, "Coupled nonlinear-damage finite element analysis and design of novel engineered wood products made of oak hardwood," *Eur. J. Wood Wood Prod.*, vol. 79, no. 1, pp. 29–47, Jan. 2021, doi: 10.1007/s00107-020-01617-7.

[12] Y. D. Murray, "Manual for LS-DYNA Wood Material Model 143," APTEK, Inc. 1257 Lake Plaza Drive Colorado Springs, CO 80906-3558, FHWA-HRT-04-097, Aug. 2007. Accessed: Jul. 27, 2024. [Online]. Available: https://www.fhwa.dot.gov/publications/research/safety/04097/04097.pdf

[13] Y. D. Murray, J. D. Reid, R. K. Faller, B. Bielenberg, and T. J. Paulsen, "Evaluation of LS-DYNA wood material model 143," United States. Federal Highway Administration, 2005.

 https://doi.org/10.52202/080513-0350